

# Virtual Corrections to the Decay $b \rightarrow s + \gamma$ <sup>1</sup>

**Christoph Greub**

*Stanford Linear Accelerator Center, Stanford University,  
Stanford, California 94309, USA*

**Tobias Hurth<sup>2</sup> and Daniel Wyler**

*Institute for Theoretical Physics, University of Zürich  
Winterthurerstr. 190, CH-8057 Zürich, Switzerland*

## Abstract

We calculate the  $O(\alpha_s)$  virtual corrections to the matrix element for  $b \rightarrow s\gamma$ , taking into account the contributions of the four-Fermi operator  $O_2$  and the electromagnetic and color dipole-type operators. The results are combined with existing  $O(\alpha_s)$  Bremsstrahlung corrections in order to obtain the relevant inclusive rate. The new result drastically reduces the large scale dependence of the leading logarithmic approximation. It implies that a very accurate prediction for the branching ratio for  $B \rightarrow X_s\gamma$  will become possible once also the corrections to the Wilson coefficients are available.

(Submitted to Physics Letters B)

---

<sup>1</sup>Work supported in part by Schweizerischer Nationalfonds and the Department of Energy, contract DE-AC03-76SF00515

<sup>2</sup>address after March 1996: ITP, SUNY at Stony Brook, Stony Brook NY 11794-3840, USA

# 1 Introduction

In the Standard model (SM) flavor-changing neutral currents only arise at the one-loop level. The corresponding B-meson decays are therefore particularly sensitive to 'new physics'; but also within the Standard model framework, they can be used to constrain several Cabibbo-Kobayashi-Maskawa matrix elements involving the top-quark. For both reasons precise experimental and theoretical work is of great importance.

$B \rightarrow K^*\gamma$  is the first rare B decay mode, which has been measured in 1993 by the CLEO collaboration [1] and recently also the first measurement of the inclusive photon energy spectrum and the branching ratio in the decay  $B \rightarrow X_s + \gamma$  was reported [2]. In contrast to the exclusive channels, the inclusive mode allows a less model-dependent comparison with theory, because no specific bound state model is needed for the final state.

This data is in a good agreement with the SM-based theoretical computations presented in [3, 4, 5] given that large uncertainties exist in both experimental and theoretical results. In particular, the measured branching ratio  $BR(B \rightarrow X_s\gamma) = (2.32 \pm 0.67) \times 10^{-4}$  [2] overlaps with the SM-based estimates in [3, 4] and in [6, 7].

As the experiments are becoming more precise in the near future, also the calculations must be refined in order to allow quantitative statements about new physics or standard model parameters.

It is well known that QCD corrections to the decay rate for  $b \rightarrow s\gamma$  bring in large logarithms of the form  $\alpha_s^n(m_W) \log^m(m_b/M)$ , where  $M = m_t$  or  $m_W$  and  $m \leq n$  (with  $n = 0, 1, 2, \dots$ ). These large terms can be resummed by renormalization group techniques. At present, only the leading logarithmic corrections (i.e.  $m = n$ ) have been calculated systematically. In this work we include one class of next-to-leading corrections which we describe in more detail below.

The calculations are most easily done in the framework of an effective theory which is obtained by integrating out the top quark and the  $W$ -boson in the standard model and other heavy particles in extensions thereof. A complete set of dimension-6 operators relevant for the process  $b \rightarrow s\gamma$  (and  $b \rightarrow s\gamma g$ ) is contained in the effective Hamiltonian [8]

$$H_{eff}(b \rightarrow s\gamma) = -\frac{4G_F}{\sqrt{2}} \lambda_t \sum_{j=1}^8 C_j(\mu) O_j(\mu) \quad , \quad (1)$$

where  $G_F$  is the Fermi constant coupling constant and  $C_j(\mu)$  are the Wilson coefficients evaluated at the scale  $\mu$ , and  $\lambda_t = V_{tb}V_{ts}^*$  with  $V_{ij}$  being the CKM matrix elements. The operators  $O_j$  read

$$\begin{aligned} O_1 &= (\bar{c}_{L\beta}\gamma^\mu b_{L\alpha}) (\bar{s}_{L\alpha}\gamma_\mu c_{L\beta}) \quad , \\ O_2 &= (\bar{c}_{L\alpha}\gamma^\mu b_{L\alpha}) (\bar{s}_{L\beta}\gamma_\mu c_{L\beta}) \quad , \\ O_7 &= (e/16\pi^2) \bar{s}_\alpha \sigma^{\mu\nu} (m_b(\mu)R + m_s(\mu)L) b_\alpha F_{\mu\nu} \quad , \\ O_8 &= (g_s/16\pi^2) \bar{s}_\alpha \sigma^{\mu\nu} (m_b(\mu)R + m_s(\mu)L) (\lambda_{\alpha\beta}^A/2) b_\beta G_{\mu\nu}^A \quad , \end{aligned} \quad (2)$$

where  $e$  and  $g_s$  are the electromagnetic and the strong coupling constants, respectively. In the magnetic moment type operators  $O_7$  and  $O_8$ ,  $F_{\mu\nu}$  and  $G_{\mu\nu}^A$  are the electromagnetic and the gluonic field strength tensors, respectively and  $L = (1 - \gamma_5)/2$  and  $R = (1 + \gamma_5)/2$  stand for the left and right-handed projection operators. We note here that the explicit mass factors in

$O_7$  and  $O_8$  are the running quark masses. We did not give explicitly the four-Fermi operators  $O_3$ – $O_6$  in eq. (2), because they have small and negligible Wilson coefficients.

To leading logarithmic precision, it is consistent to perform the matching of the effective and full theory without taking into account QCD-corrections [9] and to calculate the anomalous dimension matrix ( $8 \times 8$ ) to order  $\alpha_s$  [10]. The corresponding leading logarithmic Wilson coefficients are given explicitly in [6, 11]. The leading logarithmic contribution to the decay matrix element is then obtained by calculating the tree-level matrix element of the operator  $C_7 O_7$  and the one-loop matrix elements of the four-Fermi operators  $C_i O_i$  ( $i = 1, \dots, 6$ ). In the NDR scheme which we will use in this paper, the latter are non-zero only for  $i = 5, 6$ . Their effect can be absorbed into a redefinition of  $C_7 \rightarrow C_7^{eff}$ <sup>3</sup>

$$C_7^{eff} \equiv C_7 + Q_d C_5 + 3Q_d C_6 \quad . \quad (3)$$

Since the first order calculations contain large scale uncertainties, it is important to take into account the next-to-leading order corrections. A complete next-to-leading calculation contains two classes of improvements: First, the Wilson coefficients are required to next-leading order at the scale  $\mu \approx m_b$ . This requires the matching with the full theory (at  $\mu = m_W$ ) at the  $O(\alpha_s)$  level and the renormalization group equation has to be solved using the anomalous dimension matrix calculated up to order  $\alpha_s^2$ . Second, the real and virtual  $O(\alpha_s)$  corrections for the matrix element (at scale  $\mu \approx m_b$ ) must be evaluated.

The higher order matching has been calculated in ref. [12] and work on the Wilson coefficients is in progress. In the present paper we complete the second step. While the Bremsstrahlung corrections have been worked out [3, 4, 13, 14] in order to get a non-trivial photon energy spectrum at the partonic level for  $B \rightarrow X_s \gamma$ , the virtual corrections to  $b \rightarrow s \gamma$  have not been completely known so far. Only those virtual diagrams which are needed to cancel the infrared singularities generated by the Bremsstrahlung diagram were calculated. In the present paper we evaluate all the additional virtual correction, neglecting, as mentioned the contributions of the small operators<sup>4</sup>  $O_3$ – $O_6$ . These new contributions substantially reduce the strong scale dependence of the leading calculation.

In the following we thus consider the virtual  $O(\alpha_s)$  corrections to  $b \rightarrow s \gamma$  due to the four-Fermi operator  $O_2$  and the magnetic operators  $O_7$  (which has already been calculated in the literature) and  $O_8$  (which is new); note that the operator  $O_1$  does not contribute to the matrix elements for  $b \rightarrow s \gamma$  and  $b \rightarrow s \gamma g$  because of its color structure. As the corrections to  $O_7$  and  $O_8$  are one-loop diagrams, they are relatively easy to work out. In contrast, the corrections to  $O_2$ , involve two-loop diagrams.

## 2 Virtual Corrections to $O_2$ , $O_7$ and $O_8$

Since the virtual and Bremsstrahlung corrections to the matrix elements are only one (well-defined) part of the whole next-to-leading program, one expects that this contribution alone will depend on the renormalization scheme used. Even within the modified minimal subtraction scheme ( $\overline{MS}$ ) used here, two different “prescriptions” how to treat  $\gamma_5$ , will lead to different

---

<sup>3</sup>For the analogous  $b \rightarrow sg$  transition, the effects of the four-Fermi operators can be absorbed by the shift  $C_8 \rightarrow C_8^{eff} = C_8 + C_5$ .

<sup>4</sup>This omission will be a source of a slight scheme and scale dependence of the next-to-leading order result.

answers. Since previous calculations of the Bremsstrahlung diagrams have been done in the NDR scheme where also the leading logarithmic Wilson coefficients are available, we also use it here. A discussion of the results in the 't Hooft-Veltman scheme (HV) [15] is presented in ref. [16]. While the one-loop ( $\alpha_s^0$ ) matrix element of the operator  $O_2$  vanishes, we must consider several two-loop contributions ( $\alpha_s^1$ ) shown in Fig. 1. The diagrams in Fig. 1 are grouped in such

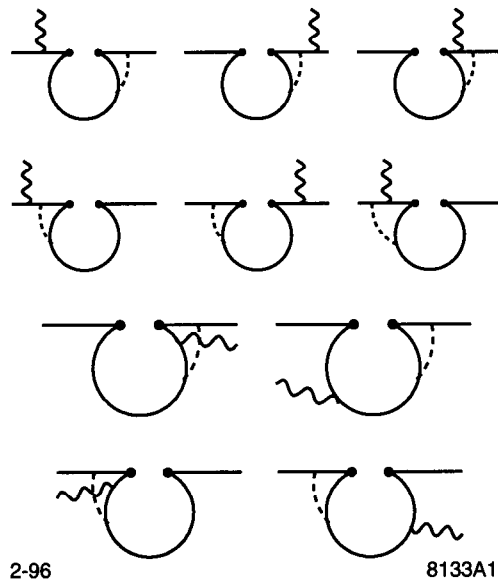


Figure 1: Non-vanishing two-loop diagrams associated with the operator  $O_2$ . The fermions ( $b$ ,  $s$  and  $c$  quark) are represented by solid lines. The wavy (dashed) line represents the photon (gluon).

a way that the sum of each line is gauge invariant. The corresponding two-loop integrals are calculated by standard Feynman parameter technique. The heart of our procedure which we explain in detail in ref. [16] is to represent the rather complicated denominators in the remaining Feynman parameter integrals as complex Mellin-Barnes integrals [17, 18, 19, 20]. After inserting this representation and interchanging the order of integration, the Feynman parameter integrals are reduced to well-known Euler beta-functions. Finally, the residue theorem allows to represent the remaining complex integral as the sum over the residues taken at the pole positions of certain beta- and gamma-functions; this naturally leads to an expansion in the ratio  $z = (m_c/m_b)^2$ , which numerically is about  $z = 0.1$ . It is, however, not a Taylor series because it also involves logarithms of  $z$ . A generic diagram which we denote by  $D$  has the form

$$D = c_0 + \sum_{n,m} c_{nm} z^n \log^m z \quad , \quad z = \frac{m_c^2}{m_b^2} \quad , \quad (4)$$

where the coefficients  $c_0$  and  $c_{nm}$  are independent of  $z$ . The power  $n$  in eq. (4) is in general a natural multiple of  $1/2$  and  $m$  is a natural number including 0. In the explicit calculation, the lowest  $n$  turns out to be  $n = 1$ . This implies the important fact that the limit  $m_c \rightarrow 0$  exists; thus, there cannot be large logarithms (if the charm quark is replaced by the up quark with its small mass) in these diagrams. As we show in [16], the power  $m$  of the logarithm is bounded by 4 independently of the value of  $n$ . We also proved that the expansion converges, at least for

$z \leq 1/4$ . In our results, we have retained all terms up to  $n = 3$ . The numerical result truncated at  $n = 3$  differs from the result for  $n = 2$  by only about 1%.

The final result for the dimensionally regularized matrix element  $M_2$  of the operator  $O_2$  which represents the sum of all two-loop diagrams in 1 is (The individual sets of diagrams are given in ref. [16].):

$$\begin{aligned}
M_2 = & \left\{ -\frac{23}{108\epsilon} \left( \frac{m_b}{\mu} \right)^{-4\epsilon} + \frac{1}{648} \left[ -833 + 144\pi^2 z^{3/2} \right. \right. \\
& + \left( 36L^3 + 108L^2 + (-324\pi^2 + 1296)L - 1296\zeta(3) - 180\pi^2 + 1728 \right) z \\
& + \left( 36L^3 + (-216\pi^2 + 432)L + 648 + 72\pi^2 \right) z^2 \\
& + \left. \left( 1092L - 756L^2 - 84\pi^2 - 54 \right) z^3 \right] \\
& + \frac{i\pi}{27} \left[ -5 + (-3\pi^2 + 45 + 9L^2 + 9L) z \right. \\
& + \left. \left. (-3\pi^2 + 9L^2)z^2 + (-12L + 28)z^3 \right] \right\} \\
& \times \frac{\alpha_s}{\pi} C_F \langle s\gamma | O_7 | b \rangle_{tree}
\end{aligned} \tag{5}$$

Note that we introduced the renormalization scale in the form  $\mu^2 \exp(\gamma_E)/(4\pi)$  which is convenient for  $\overline{MS}$  subtraction. Here,  $z = (m_c/m_b)^2$  and  $L = \log(z)$  and  $\epsilon$  is the ultraviolet regulator in the convention, where  $d = 4 - 2\epsilon$ . The symbol  $\zeta$  in eq. (5) denotes the Riemann Zeta function, with  $\zeta(3) \approx 1.2021$ ;  $C_F = 4/3$  is a color factor and the matrix element  $\langle s\gamma | O_7 | b \rangle_{tree}$  is the  $O(\alpha_s^0)$  tree level matrix element of the operator  $O_7$ . In eq. (5) we have inserted the numerical values for the charges of the up and down type quarks ( $Q_u = 2/3$  and  $Q_d = -1/3$ ).

There are also counterterms to be included. As we are interested in contributions to  $b \rightarrow s\gamma$  which are proportional to  $C_2$ , we have to take, in addition to the two-loop matrix elements of  $C_2 O_2$ , also the one-loop matrix elements of the four Fermi operators  $C_2 \delta Z_{2j} O_j$  ( $j = 1, \dots, 6$ ) and the tree level contribution of the magnetic operator  $C_2 \delta Z_{27} O_7$ . In the NDR scheme the only non-vanishing contributions to  $b \rightarrow s\gamma$  come from  $j = 5, 6, 7$ . The operator renormalization constants  $Z_{ij}$  can be extracted from the literature [10] in the context of the leading order anomalous dimension matrix:

$$\begin{aligned}
\delta Z_{25} &= -\frac{\alpha_s}{48\pi\epsilon} C_F \quad , \quad \delta Z_{26} = \frac{\alpha_s}{16\pi\epsilon} C_F \quad , \\
\delta Z_{27} &= \frac{\alpha_s}{16\pi\epsilon} (6Q_u - \frac{8}{9}Q_d) C_F \quad .
\end{aligned} \tag{6}$$

Defining

$$M_{2j} = \langle s\gamma | \delta Z_{2j} O_j | b \rangle \quad , \tag{7}$$

we find the following contributions to the matrix elements

$$\begin{aligned}
M_{25} &= -\frac{\alpha_s}{48\pi} Q_d C_F \frac{1}{\epsilon} \left( \frac{m_b}{\mu} \right)^{-2\epsilon} \langle s\gamma | O_7 | b \rangle_{tree} \\
M_{26} &= \frac{3\alpha_s}{16\pi} Q_d C_F \frac{1}{\epsilon} \left( \frac{m_b}{\mu} \right)^{-2\epsilon} \langle s\gamma | O_7 | b \rangle_{tree} \\
M_{27} &= \frac{\alpha_s}{\pi} \left( \frac{3Q_u C_F}{8} - \frac{Q_d C_F}{18} \right) \frac{1}{\epsilon} \langle s\gamma | O_7 | b \rangle_{tree}
\end{aligned} \tag{8}$$

We note that there is no one-loop contribution to  $b \rightarrow s\gamma$  from the counterterm proportional to  $(C_2 \frac{1}{\epsilon} O_{12}^{ev})$ , where the evanescent operator  $O_{12}^{ev}$  (see e.g. the last ref. in [10]) reads

$$O_{12}^{ev} = \frac{1}{6} O_2 (\gamma_\mu \rightarrow \gamma_{[\mu} \gamma_\nu \gamma_{\rho]}) - O_2 \quad . \quad (9)$$

Adding the two-loop expression  $M_2$  (eq.(5)) and the counterterms (eq. (8)), we find the renormalized result, which can be written as

$$M_2^{ren} = \langle s\gamma | O_7 | b \rangle_{tree} \frac{\alpha_s}{4\pi} \left( \ell_2 \log \frac{m_b}{\mu} + r_2 \right) \quad , \quad (10)$$

with

$$\ell_2 = \frac{416}{81} \quad . \quad (11)$$

$$\begin{aligned} \Re r_2 = & \frac{2}{243} \left\{ -833 + 144\pi^2 z^{3/2} \right. \\ & + \left[ 1728 - 180\pi^2 - 1296\zeta(3) + (1296 - 324\pi^2)L + 108L^2 + 36L^3 \right] z \\ & + \left[ 648 + 72\pi^2 + (432 - 216\pi^2)L + 36L^3 \right] z^2 \\ & \left. + \left[ -54 - 84\pi^2 + 1092L - 756L^2 \right] z^3 \right\} \quad (12) \end{aligned}$$

$$\Im r_2 = \frac{16\pi}{81} \left\{ -5 + \left[ 45 - 3\pi^2 + 9L + 9L^2 \right] z + \left[ -3\pi^2 + 9L^2 \right] z^2 + \left[ 28 - 12L \right] z^3 \right\} \quad (13)$$

Here,  $\Re r_2$  and  $\Im r_2$  denote the real and the imaginary part of  $r_2$ , respectively.

The virtual corrections associated with the operator  $O_7$  have been taken into account by Ali and Greub, see e.g. [3, 4, 13]. These corrections contain infrared singularities and for  $m_s = 0$  also collinear singularities. At the level of the decay rate, these singularities cancel if one adds the Bremsstrahlung correction based on the matrix element squared of the operator  $O_7$ . Denoting by  $\Gamma_{77}$  the sum of the lowest order contribution, the virtual  $O(\alpha_s)$  correction and those parts of the Bremsstrahlung correction just mentioned, this finite quantity reads in the limit  $m_s = 0$

$$\Gamma_{77} = \Gamma_{77}^0 \left[ 1 + \frac{\alpha_s}{3\pi} \left( \frac{16}{3} - \frac{4\pi^2}{3} + 4 \log \frac{m_b}{\mu} \right) \right] \quad , \quad (14)$$

where the lowest order contribution  $\Gamma_{77}^0$  is given by

$$\Gamma_{77}^0 = \frac{m_b^2(\mu) m_b^3}{32\pi^4} |G_F \lambda_t C_7^{eff}|^2 \alpha_{em} \quad . \quad (15)$$

For later convenience, it is useful to define a 'modified' matrix element for  $b \rightarrow s\gamma$ , in such a way that its square reproduces the result in eq. (14). This modified matrix element  $M_7^{mod}$  reads

$$M_7^{mod} = \langle s\gamma | O_7 | b \rangle_{tree} \left( 1 + \frac{\alpha_s}{4\pi} \left( \ell_7 \log \frac{m_b}{\mu} + r_7 \right) \right) \quad (16)$$

with

$$\ell_7 = \frac{8}{3} \quad , \quad r_7 = \frac{8}{9} (4 - \pi^2) \quad . \quad (17)$$

Finally, we consider the contributions to  $b \rightarrow s\gamma$  generated by the operator  $O_8$ , i. e., the matrix element

$$M_8 = \langle s\gamma | O_8 | b \rangle . \quad (18)$$

The corresponding Feynman diagrams are shown in Fig. 2. The sum of all 6 diagrams in Fig.2

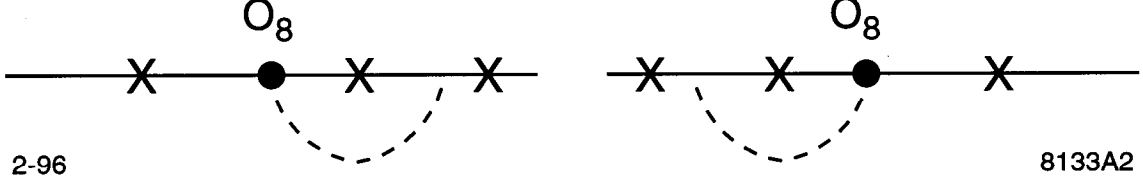


Figure 2: Contributions of  $O_8$  to  $b \rightarrow s\gamma$ . The cross (x) denotes the possible place where the photon is emitted.

yields

$$M_8 = \frac{Q_d C_F \alpha_s}{12 \pi} \left[ -\frac{12}{\epsilon} - 33 + 2\pi^2 + 24 \log(m_b/\mu) - 6i\pi \right] \langle s\gamma | O_7 | b \rangle_{tree} . \quad (19)$$

There is also a contribution from a counterterm, reading

$$M_8(\text{counter}) = \delta Z_{87} \langle s\gamma | O_7 | b \rangle_{tree} , \quad (20)$$

where the renormalization constant

$$\delta Z_{87} = \frac{\alpha_s}{\pi} C_F Q_d \frac{1}{\epsilon} \quad (21)$$

can again be taken from the literature [10]. We thus arrive at the renormalized result  $M_8$ :

$$M_8^{ren} = \langle s\gamma | O_7 | b \rangle_{tree} \frac{\alpha_s}{4\pi} \left( \ell_8 \log \frac{m_b}{\mu} + r_8 \right) , \quad (22)$$

with

$$\ell_8 = -\frac{32}{9} , \quad r_8 = -\frac{4}{27} (-33 + 2\pi^2 - 6i\pi) . \quad (23)$$

### 3 Impact on the branching ratio

To summarize, we have calculated the virtual corrections to  $b \rightarrow s\gamma$  coming from the operators  $O_2$ ,  $O_7$  and  $O_8$ . The contributions from the other operators in eq. (1) are either small or vanish. As discussed above, some of the Bremsstrahlung corrections to the operator  $O_7$  have been transferred into the matrix element  $M_7^{mod}$  for  $b \rightarrow s\gamma$  in order to simplify the following discussion. While we have neglected those virtual corrections of the operators  $O_3$ - $O_6$  which are given by the analogous diagrams as shown in Fig. 1, we took into account the non-vanishing diagrams of  $O_5$  and  $O_6$  where the gluon connects the external quark lines and the photon is radiated from the charm quark; these corrections are automatically taken into account when using  $C_7^{eff}$  instead of  $C_7$ . Since the Wilson coefficients of the omitted operators are about fifty

times smaller than that of the leading one and since we expect that their matrix elements can be enhanced at most by color factors, it seems reasonable to neglect them.

We can now easily write down the amplitude  $A(b \rightarrow s\gamma)$  for  $b \rightarrow s\gamma$  by summing the various contributions derived in the previous section. We follow closely the treatment of Buras et al. [6], where the general structure of the next-to-leading order result is discussed in detail. We write

$$A(b \rightarrow s\gamma) = -\frac{4G_F\lambda_t}{\sqrt{2}} \hat{D} \langle s\gamma | O_7(\mu) | b \rangle_{tree} \quad (24)$$

with  $\hat{D}$

$$\hat{D} = C_7^{eff}(\mu) + \frac{\alpha_s(\mu)}{4\pi} \left( C_i^{(0)eff}(\mu) \ell_i \log \frac{m_b}{\mu} + C_i^{(0)eff} r_i \right) \quad , \quad (25)$$

and where the quantities  $\ell_i$  and  $r_i$  are given for  $i = 2, 7, 8$  in eqs. (11,12), (17) and (23), respectively. The first term,  $C_7^{eff}(\mu)$ , on the rhs of eq. (25) has to be taken up to next-to-leading logarithmic precision in order to get the full next-to-leading logarithmic result, whereas it is sufficient to use the leading logarithmic values of the other Wilson coefficients in eq. (25). As the next-to-leading coefficient  $C_7^{eff}$  is not known yet, we replace it in the numerical evaluation by its leading logarithmic value  $C_7^{(0)eff}$ . The notation  $\langle s\gamma | O_7(\mu) | b \rangle_{tree}$  in eq. (24) indicates that the explicit  $m_b$  factor in the operator  $O_7$  is the running mass taken at the scale  $\mu$ .

Since the relevant scale for a  $b$  quark decay is expected to be  $\mu \sim m_b$ , we expand the matrix elements of the operators around  $\mu = m_b$  up to order  $O(\alpha_s)$ . The result is

$$A(b \rightarrow s\gamma) = -\frac{4G_F\lambda_t}{\sqrt{2}} D \langle s\gamma | O_7(m_b) | b \rangle_{tree} \quad (26)$$

with  $D$

$$D = C_7^{eff}(\mu) + \frac{\alpha_s(m_b)}{4\pi} \left( C_i^{(0)eff}(\mu) \gamma_{i7}^{(0)eff} \log \frac{m_b}{\mu} + C_i^{(0)eff} r_i \right) \quad , \quad (27)$$

where the quantities  $\gamma_{i7}^{(0)eff} = \ell_i + 8\delta_{i7}$  are just the entries of the (effective) leading order anomalous dimension matrix [6]. As also pointed out in this reference, the explicit logarithms of the form  $\alpha_s(m_b) \log(m_b/\mu)$  in eq. (27) are cancelled by the  $\mu$ -dependence of  $C_7^{(0)eff}(\mu)$ .<sup>5</sup> Therefore the scale dependence is significantly reduced by including the virtual corrections calculated in this paper.

The decay width  $\Gamma^{virt}$  which follows from  $A(b \rightarrow s\gamma)$  in eq. (26) reads

$$\Gamma^{virt} = \frac{m_{b,pole}^5 G_F^2 \lambda_t^2 \alpha_{em}}{32\pi^4} F |D|^2 \quad , \quad (28)$$

where in fact we discard the term of  $O(\alpha_s^2)$  in  $|D|^2$ . The factor  $F$  in eq. (28) is

$$F = \left( \frac{m_b(\mu = m_b)}{m_{b,pole}} \right)^2 = 1 - \frac{8}{3} \frac{\alpha_s(m_b)}{\pi} \quad . \quad (29)$$

To get the inclusive decay width for  $b \rightarrow s\gamma(g)$ , also the Bremsstrahlung corrections (except the part we have already absorbed) must be added. The contribution of the operators  $O_2$  and

<sup>5</sup>As we neglect the virtual correction of  $O_3$ - $O_6$ , there is a small left-over  $\mu$  dependence.

$O_7$  have been calculated before by Ali and Greub [3], recently also the complete set has been worked out [4, 13, 14]. In the present work we neglect the small contribution of the operators  $O_3 - O_6$  in analogy to the virtual corrections, where only  $O_2$ ,  $O_7$  and  $O_8$  were considered also.

The branching ratio  $\text{BR}(b \rightarrow s\gamma(g))$  is then obtained by deviding the decay width  $\Gamma = \Gamma^{\text{virt}} + \Gamma^{\text{brems}}$  for  $b \rightarrow s\gamma(g)$  by the theoretical expression for the semileptonic width  $\Gamma_{sl}$  (including the well-known  $O(\alpha_s)$  radiative corrections [21]) and by multiplying with the measured semileptonic branching ratio  $\text{BR}_{sl} = (10.4 \pm 0.4)\%$  [22].

In Fig. 3 we present the result for the branching ratio for  $b \rightarrow s\gamma(g)$  based on the contributions discussed above. A rather crucial parameter is the ratio  $m_c/m_b$ ; it enters both,  $b \rightarrow s\gamma$  mainly through the virtual corrections of  $O_2$  and the semileptonic decay width through phase space. To estimate this ratio we put  $m_{b,\text{pole}} = 4.8 \pm 0.15$  GeV for the  $b$  quark pole mass; from the mass difference  $m_b - m_c = 3.40$  GeV, which is known quite precisely through the  $1/m_Q$  expansion [23, 24], one then gets  $m_c/m_b = 0.29 \pm 0.02$ . In the curves we have used the central values for  $m_{b,\text{pole}}$  and  $m_c/m_b$ . For the CKM matrix elements we put  $V_{cb} = V_{ts}$  and  $V_{tb} = 1$ . In Fig. 3 we have plotted the calculated branching ratio as a function of the top quark mass  $m_t$ . The horizontal dotted curves show the CLEO limits for the branching ratio  $\text{BR}(B \rightarrow X_s\gamma)$  [2]. To illustrate the scale dependence of the branching ratio, we varied the scale  $\mu$  between  $(m_b/2)$

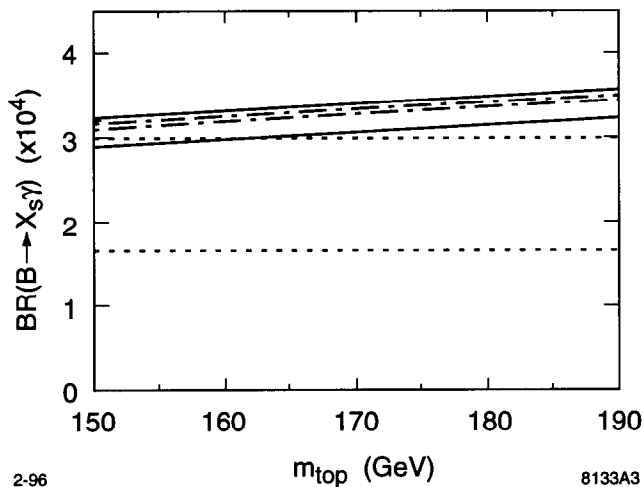


Figure 3: Branching ratio for  $b \rightarrow s\gamma(g)$  based on the formulae in this section. The different curves are explained in the text.

and  $(2m_b)$ . We considered two 'scenarios' which differ by higher order terms. First, we put the scale  $\mu = m_b$  in the explicit  $\alpha_s$  factor in eq. (27) and in the correction to the semileptonic decay width, as it was also done by Buras et al. [6]. The resulting  $\mu$  dependence is shown by dash-dotted lines. Second, we retain the scale  $\mu$  in the explicit  $\alpha_s$  factors; this leads to the solid curves in Fig. 3. In both cases the upper curve corresponds to  $\mu = m_b/2$  and the lower curve to  $\mu = 2m_b$ . We mention that the  $\mu$ -band is larger in the second scenario and it is therefore safer to use this band to illustrate the remaining scale uncertainties.

In Fig. 4 we show for comparison the leading logarithmic result for the branching ratio for  $b \rightarrow s\gamma$ , based on the tree-level matrix element of the operator  $O_7$  and using the tree-level formula for the semileptonic decay width. Varying the scale  $\mu$  in the same range as above, leads to the dash-dotted curves in Fig. 4. We have also plotted the result as it was available

before the inclusion of the virtual corrections of  $O_2$  and  $O_8$  (but with Bremsstrahlung and virtual corrections to  $O_7$  included). This is reproduced by putting  $\ell_2 = r_2 = \ell_8 = r_8 = 0$  in our formulae. As noticed in the literature [3, 14], the  $\mu$  dependence in this case (solid lines) is even larger than in the leading logarithmic result.

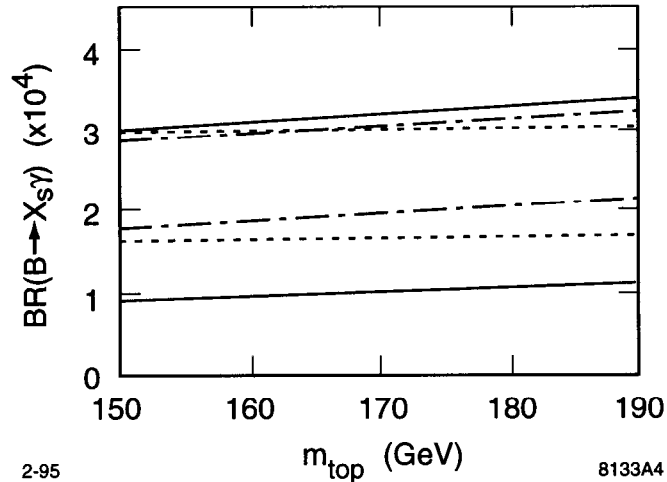


Figure 4: Branching ratio for  $b \rightarrow s\gamma(g)$ . The leading logarithmic result is shown by the dash-dotted curve; The solid line shows the situation before the virtual contributions of  $O_2$  and  $O_8$ . See text.

From the results in Fig. 4 it was relatively easy to read off a reasonable prediction for the branching ratio within a large error which was essentially determined by the  $\mu$  dependence. In the improved calculation (Fig. 3) the  $\mu$  dependence is significantly reduced, because all the logarithms of the form  $\alpha_s(m_b) \log(m_b/\mu)$  are cancelled as discussed above. In the present situation it is, however, premature to extract a prediction for the branching ratio from Fig. 3. This only will be possible when also  $C_7^{eff}$  is known up to next-to-leading logarithmic precision. But this result will, essentially, shift the narrow bands of Fig. 3, without broadening them significantly. Thus, a very precise prediction will become possible and renewed experimental efforts will be required. It is, however, rewarding to see that the next-to-leading result will lead to a strongly improved determination of the standard model parameters or to better limits to new physics.

**Acknowledgements** Discussions with A. Ali, S. Brodsky, M. Lautenbacher, M. Peskin and L. Reina are thankfully acknowledged. We are particularly indebted to M. Misiak for many useful comments; especially his remarks concerning the renormalization scale dependence were extremely useful. One of us (C.G.) would like to thank the Institute for Theoretical Physics in Zürich for the kind hospitality.

## References

- [1] R. Ammar et al. (CLEO Collaboration), Phys. Rev. Lett. **71** (1993) 674.
- [2] M.S. Alam et al. (CLEO Collaboration), Phys. Rev. Lett. **74** (1995) 2885.
- [3] A. Ali and C. Greub, Z. Phys. **C49** (1991) 431; Phys. Lett. **B259** (1991) 182.  
A. Ali and C. Greub, Phys. Lett. **B287** (1992) 191.  
A. Ali and C. Greub, Z. Phys. **C60** (1993) 433.
- [4] A. Ali and C. Greub, Phys. Lett. **B361** (1995) 146.
- [5] R.D. Dikeman, M. Shifman, and R.G. Uraltsev, Preprint TPI-MINN-95/9-T, UMN-TH-1339-95, UND-HEP-95-BIG05 (hep-ph/9505397).
- [6] A.J. Buras, M. Misiak, M. Münz, and S. Pokorski, Nucl. Phys. **B424** (1994) 374.
- [7] M. Ciuchini et al., Phys. Lett. **B334** (1994) 137.
- [8] B. Grinstein, R. Springer, and M.B. Wise, Phys. Lett. **202** (1988) 138; Nucl Phys. **B339** (1990) 269.
- [9] T. Inami and C.S. Lim, Prog. Theor. Phys. **65** (1981) 297.
- [10] M. Ciuchini et al., Phys. Lett. **B316** (1993) 127; Nucl. Phys. **B415** (1994) 403;  
G. Cella et al., Phys. Lett. **B325** (1994) 227.  
M. Misiak, Nucl. Phys. **B393** (1993) 23; Erratum ibid. **B439** (1995) 461.
- [11] A. Ali, G. Giudice, and T. Mannel, Z. Phys. **C67** (1995) 417.
- [12] K. Adel and Y.-p. Yao, Phys. Rev. **D49** (1994) 4945.
- [13] A. Ali and C. Greub, in preparation.
- [14] N. Pott, preprint Tech. Univ. Munich, TUM-T31-93/95 (hep-ph/9512252).
- [15] G. 't Hooft and M. Veltman, Nucl. Phys. **B44** (1972) 189.
- [16] C. Greub, T. Hurth and D. Wyler, in preparation.
- [17] E.E. Boos and A.I. Davydychev, Theor. Math. Phys. **89** (1992) 1052.
- [18] N.I. Usyukina, Theor. Math. Phys. **79** (1989) 385, **22** (1975) 211.
- [19] V.A. Smirnov, Renormalization and Asymptotic Expansions, Birkhäuser Basel 1991.
- [20] A. Erdelyi (ed.), Higher Transcendental Functions, McGraw New York 1953.
- [21] G. Corbo, Nucl. Phys. **B212** (1983) 99; N. Cabibbo, G. Corbo, and L. Maiani, it ibid. **B155** (1979) 93.
- [22] L. Gibbons (CLEO Collaboration), in Proceedings of the XXX Rencontres de Moriond, Les Arcs, March 1994.

- [23] I. Bigi et al., Phys. Rev. Lett. **71** (1993) 496.
- [24] M. Shifman, N.G. Uraltsev, and A. Vainshtein, Phys. Rev. **D51** (1995) 2217;  
M.B. Voloshin, TPI-MINN-94/38-T (hep-ph/9411296).